



# Multifunctional quinoxaline-hydrazone derivatives with acetylcholinesterase and monoamine oxidases inhibitory activities as potential agents against Alzheimer's disease

Ulviye Acar Çevik<sup>1,2</sup> · Derya Osmaniye<sup>1,2</sup> · Begüm Nurpelin Sağlık<sup>1,2</sup> · Betül Kaya Çavuşoğlu<sup>1,2</sup> · Serkan Levent<sup>1,2</sup> · Abdullah Burak Karaduman<sup>3</sup> · Sinem Ilgin<sup>3</sup> · Ahmet Çağrı Karaburun<sup>1</sup> · Yusuf Özkay<sup>1,2</sup> · Zafer Asım Kaplancıklı<sup>1</sup> · Gülhan Turan<sup>1</sup>

Received: 19 January 2020 / Accepted: 31 March 2020  
© Springer Science+Business Media, LLC, part of Springer Nature 2020

## Abstract

Multitarget molecules are considered as an effective way for the treatment of AD, instead of the classic one-drug-one-target strategy because of the multifactorial nature of AD. A variety of studies indicate that several enzymes inhibitors can be useful in the treatment of AD, including acetylcholinesterase (AChE), butyrylcholinesterase (BuChE) and monoamine oxidase (MAO). Various substituted quinoxaline-hydrazone derivatives were synthesized, and their activity in vitro were investigated, including AChE/BuChE inhibitory activity and MAOA/B inhibitory activity. Based on the experimental results, compound **5I** exhibited good inhibitory potency on both AChE ( $IC_{50} = 0.028 \pm 0.001 \mu M$ ) and monoamine oxidase B ( $IC_{50} = 0.046 \pm 0.002 \mu M$ ). Molecular modeling studies showed that **5I** could bind to the active site of AChE and MAO-B. Taken together, these results suggested that compound **5I** might be a potential multifunctional agent for the treatment of AD.

**Keywords** Quinoxaline-hydrazone · Acetylcholinesterase · Butyrylcholinesterase · Monoamine oxidases · Enzyme inhibition

## Introduction

The potential targets have been comprehensively studied for several years in the therapy of psychiatric and neurodegenerative diseases with complex and variable underlying mechanisms. Current therapeutic strategies have favored drugs that act on a single molecular target while new pharmacological approaches aim candidate compounds designed to interact with multiple neural and biochemical targets. Since the multifactorial nature of Alzheimer's disease (AD), the administration of a multi-targeted drug in the

treatment might provide improved symptomatic efficacy and eliminate the use of several drugs with potentially different degrees of bioavailability, pharmacokinetics, and metabolism (Youdim and Buccafusco 2005; Li et al. 2017).

The etiology of AD is not completely known, but low levels of acetylcholine (ACh),  $\beta$ -amyloid deposits, dyshomeostasis of biometals and oxidative stress have been thought to play significant roles in the pathogenesis of the disease (Scarpini et al. 2003). The cholinergic hypothesis suggests that the inhibition of acetylcholinesterase (AChE) increase the levels of ACh and treat some symptoms of AD patients (Xiao et al. 2017). Therefore, AChE inhibitors such as donepezil, rivastigmine, and galantamine are the clinical first-line drugs in the therapy of AD. Though these drugs provide improvement in memory and cognitive function, fail to achieve a comprehensive and satisfactory therapeutic solution (Takeda et al. 2006; Raina et al. 2008).

Monoamine oxidase (MAO) is responsible for catalysing the oxidative deamination of a variety of biogenic and xenobiotic amines and considered to be also an important target in the treatment of AD (Youdim et al. 2006). The inhibition of MAO prevents the formation of neurotoxic

✉ Ulviye Acar Çevik  
uacar@anadolu.edu.tr

<sup>1</sup> Department of Pharmaceutical Chemistry, Faculty of Pharmacy, Anadolu University, Eskişehir, Turkey  
<sup>2</sup> Doping and Narcotic Compounds Analysis Laboratory, Faculty of Pharmacy, Anadolu University, Eskişehir, Turkey  
<sup>3</sup> Department of Pharmaceutical Toxicology, Faculty of Pharmacy, Anadolu University, Eskişehir, Turkey

products, such as hydrogen peroxide and aldehydes, which are known to be related with neurodegenerative diseases, thus MAO inhibitors protect the nerve cells from oxidative damage and neurotoxicity (Xu et al. 2018). MAOs are flavin adenine dinucleotide (FAD)-containing enzymes and have two functional isozymic forms, namely, MAO-A and MAO-B, based on their substrate and inhibitor specificities (Edmondson et al. 2004). MAO-A inhibitors are used as clinical antidepressants and anti-anxiety agents, while MAO-B inhibitors are employed in the therapy of neurodegenerative disorders such as AD and Parkinson's diseases (PD) (Wouters 1998; Youdim et al. 2006). Selegiline, an irreversible and selective MAO-B inhibitor, has been reported as an effective drug in individuals with AD due to its neuroprotective property (Bar-Am et al. 2010).

The strategy targeting the simultaneous inhibition of MAO and AChE represents one of the promising approaches due to the multifactorial pathogenesis of AD. Lately, ladostigil was designed via the combination of pharmacophores of rivastigmine (an AChE inhibitor) and rasagiline (an MAO inhibitor) to give a novel dual AChE and MAO-B inhibitor for the therapy of AD and approved for Phase II clinical trials by the FDA (Fig. 1) (Sterling et al. 2002). Attempts to design a molecule with anti-MAO and anti-AChE activities have previously been reported (Sterling et al. 2002; Sang et al. 2017a, 2017b).

Quinoxalines has become an important construction motif for the development of new drugs. In particular, quinoxaline derivatives have multitude of pharmacological actions including MAO and AChE inhibitory properties (Khattab et al. 2015, 2010; Huang et al. 2011). On the other hand, hydrazone derivatives have been also documented as promising scaffold to design anti-MAO and anti-AChE agents (Evrans-Aksöz et al. 2015; Tripathi and Ayyannan 2016; D'Ascenzio et al. 2015; Dias Viegas et al. 2018; Karaman et al. 2016). In an attempt to develop novel MAO and AChE inhibitory agents, in present study, we combined hydrazone moiety and quinoxaline ring to synthesize multifunctional agents for the potential treatment of AD. The mode of inhibition and interaction modes of the most active inhibitors were explored via kinetic and reversibility studies along with docking studies.

## Material and methods

### Chemistry

All chemicals used in the syntheses were purchased either from Merck Chemicals (Merck KGaA, Darmstadt, Germany) or Sigma-Aldrich Chemicals (Sigma-Aldrich Corp., St. Louis, MO, USA). The reactions and the purities of the compounds were observed by thin layer chromatography (TLC) on silica gel 60 F254 aluminum sheets obtained from Merck (Darmstadt, Germany). Melting points of the synthesized compounds were recorded by MP90 digital melting point apparatus (Mettler Toledo, OH, USA) and were presented as uncorrected.  $^1\text{H}$  NMR and  $^{13}\text{C}$  NMR spectra were recorded by a Bruker 300 MHz and 75 MHz digital FT-NMR spectrometer (Bruker Bioscience, Billerica, MA, USA) in DMSO- $d_6$ , respectively. In the NMR spectra splitting patterns were designated as follows: s: singlet; d: doublet; t: triplet; m: multiplet. Coupling constants (J) were reported as Hertz. LC-MS-MS studies were performed on a Shimadzu, 8040 LCMSMS spectrophotometer (Shimadzu, Tokyo, Japan).

#### Microwave-assisted synthesis of quinoxaline-2(1H)-one (1)

1,2-Phenylenediamine (5.4 g, 0.05 mol) and ethyl glyoxalate (6.2 mL, 0.06 mol) were reacted in a vial (30 mL) of microwave synthesis reactor (Anton-Paar Monowave 300) in ethanol. The reaction was maintained under the conditions of 200 °C and 25 bar for 15 min. After this time, the reaction mixture was cooled and the solvent was evaporated. The residue was washed with water, dried and recrystallized from ethanol (Yan-Yan 2010).

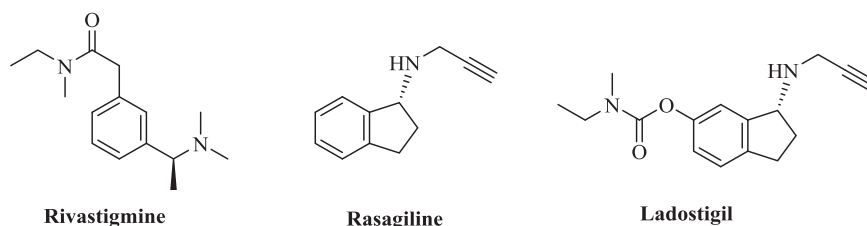
#### Synthesis of 2-chloroquinoxaline (2)

Quinoxaline-2(1H)-one (1) (5.6 g, 0.038 mol) was refluxed for 3 h in  $\text{POCl}_3$  (100 mL). After cooling, excessive of  $\text{POCl}_3$  was evaporated and crude product was held for further reaction without recrystallization (Becker 2008).

#### Microwave-assisted synthesis of quinoxaline-2-hydrazine (3)

2-Chloroquinoxaline (2) (4.7 g, 0.029 mol) were reacted with hydrazine hydrate (99%) (3.5 mL) in tetrahydrofuran

**Fig. 1** Chemical structures of rivastigmine, rasagiline and ladostigil



(THF) (10 mL) at 170 °C and 10 bar for 15 min in a vial (30 mL) of microwave synthesis reactor (Anton-Paar Monowave 300). In the end of reaction, the solvent and excessive of hydrazine hydrate were evaporated, the residue was washed with water, dried and recrystallized from ethanol (Chen et al. 2008).

### Synthesis of benzaldehyde derivatives (4a–4m)

Appropriate seconder amines (5 mmol) and 4-fluorobenzaldehyde (5 mmol, 0.62 g) were refluxed in dimethylformamide (10 mL) with the presence of potassium carbonate (6 mmol, 0.83 g). After TLC screening, the mixture was poured into ice water and filtered. The products were recrystallized from ethanol (Osmaniye et al. 2019).

### General synthesis of N-(4-substitutedbenzylidene)-N'-quinoxalin-2-yl-hydrazine derivatives (5a–5m)

Quinoxaline-2-hydrazine (3) (0.32 g, 2 mmol) and appropriate benzaldehyde derivatives (4a–4m) (2 mmol) in ethanol (25 mL) were refluxed for 1 h with catalytic amount of acetic acid. The precipitate was filtered, dried and recrystallized from ethanol (Kaya Çavuşoğlu et al. 2018a).

**2-[2-(4-(Pyrrolidin-1-yl)benzylidene)hydrazineyl]quinoxaline (5a)** Yield 79%, m.p. 276.2–278.0 °C. IR  $\nu_{\max}$  (cm<sup>-1</sup>): 3685 (N–H) 3035 (aromatic C–H), 2972 (aliphatic C–H), 1610–1427 (C=N, C=C), 1350–1020 (C–N). <sup>1</sup>H NMR (300 Mhz, DMSO-d<sub>6</sub>, ppm)  $\delta$  1.96 (4H, br.s, pyrrolidin-H), 3.27 (4H, br s, pyrrolidine-H), 6.57 (2H, d, *J* = 8.6 Hz, 1,4-disubstituted benzene), 7.40–7.47 (1H, m, quinoxaline), 7.55 (2H, d, *J* = 8.6 Hz, aromatic-H, 1,4-disubstituted benzene), 7.63 (2H, d, *J* = 3.7 Hz, quinoxaline), 7.87 (1H, d, *J* = 8.2 Hz, quinoxaline), 8.01 (1H, s, quinoxaline), 9.02 (1H, s, N=CH), 11.35 (1H, s, NH). <sup>13</sup>C NMR (75 MHz, DMSO-d<sub>6</sub>, ppm)  $\delta$  25.43 (pyrrolidine-CH<sub>2</sub>), 47.70 (pyrrolidine-CH<sub>2</sub>), 112.08 (1,4-disubstituted benzene-CH), 121.90 (quinoxaline-CH), 124.96 (1,4-disubstituted benzene-C), 126.35 (quinoxaline-CH), 128.42 (quinoxaline-CH), 129.19 (1,4-disubstituted benzene-CH), 130.64 (quinoxaline-CH), 136.99 (quinoxaline-CH), 138.05 (quinoxaline-C), 141.71 (quinoxaline-C), 143.72 (CH=N), 148.86 (1,4-disubstituted benzene-C), 150.84 (quinoxaline-C). HRMS (m/z): [M+H]<sup>+</sup> calcd for C<sub>19</sub>H<sub>19</sub>N<sub>5</sub>: 318.1713; found: 318.1699.

**2-[2-(4-(Piperidin-1-yl)benzylidene)hydrazineyl]quinoxaline (5b)** Yield 75%, m.p. 252.1–254.2 °C. IR  $\nu_{\max}$  (cm<sup>-1</sup>): 3176 (N–H) 3057 (aromatic C–H), 2935 (aliphatic C–H), 1606–1450 (C=N, C=C), 1307–1111 (C–N). <sup>1</sup>H NMR (300 Mhz, DMSO-d<sub>6</sub>, ppm)  $\delta$  1.59 (6H, s, piperidine-H),

3.25 (4H, br s, piperidine-H), 6.97 (2H, d, *J* = 8.7 Hz, 1,4-disubstituted benzene), 7.42–7.48 (1H, m, quinoxaline), 7.58 (2H, d, *J* = 8.7 Hz, 1,4-disubstituted benzene), 7.64–7.66 (2H, m, quinoxaline), 7.89 (1H, d, *J* = 8.1 Hz, quinoxaline), 8.03 (1H, s, quinoxaline), 9.03 (1H, s, N=CH), 11.43 (1H, s, NH). <sup>13</sup>C NMR (75 MHz, DMSO-d<sub>6</sub>, ppm)  $\delta$  24.39, 25.48, 49.08, 115.34, 124.51, 125.12, 126.43, 128.17, 129.21, 130.67, 136.96, 138.14, 141.63, 143.06, 150.83, 152.42. HRMS (m/z): [2M+2H]<sup>+</sup> calcd for C<sub>20</sub>H<sub>21</sub>N<sub>5</sub>: 166.5971; found: 166.5966.

**2-[2-(4-(2-Methylpiperidin-1-yl)benzylidene)hydrazineyl]quinoxaline (5c)** Yield 72%, m.p. 225.9–227.4 °C. IR  $\nu_{\max}$  (cm<sup>-1</sup>): 3199 (N–H) 3043 (aromatic C–H), 2935 (aliphatic C–H), 1606–1490 (C=N, C=C), 1307–1109 (C–N). <sup>1</sup>H NMR (300 Mhz, DMSO-d<sub>6</sub>, ppm)  $\delta$  1.01 (3H, d, *J* = 6.7 Hz, CH<sub>3</sub>), 1.57–1.76 (6H, m, piperidine-H), 2.89 (1H, t, *J* = 12.2 Hz, piperidine-H), 3.47 (1H, d, *J* = 12.7 Hz, piperidine-H), 4.18–4.21 (1H, m, piperidine-H), 6.93 (2H, d, *J* = 8.9 Hz, 1,4-disubstituted benzene), 7.42–7.48 (1H, m, quinoxaline), 7.57 (2H, d, *J* = 8.9 Hz, 1,4-disubstituted benzene), 7.64–7.65 (2H, m, quinoxaline), 7.88 (1H, d, *J* = 8.1 Hz, quinoxaline), 8.02 (1H, s, quinoxaline), 9.03 (1H, s, N=CH), 11.42 (1H, s, NH). <sup>13</sup>C NMR (75 MHz, DMSO-d<sub>6</sub>, ppm)  $\delta$  13.35 (CH<sub>3</sub>), 18.74, 25.86, 30.90, 42.04, 49.32, 115.22, 124.03, 125.09, 126.42, 128.24, 129.20, 130.66, 136.96, 138.13, 141.65, 143.13, 150.84, 151.74. HRMS (m/z): [M+H]<sup>+</sup> calcd for C<sub>21</sub>H<sub>23</sub>N<sub>5</sub>: 346.2026; found: 346.2016.

**2-[2-(4-(3-Methylpiperidin-1-yl)benzylidene)hydrazineyl]quinoxaline (5d)** Yield 69%, m.p. 218.2–219.7 °C. IR  $\nu_{\max}$  (cm<sup>-1</sup>): 3211 (N–H) 3055 (aromatic C–H), 2951 (aliphatic C–H), 1608–1492 (C=N, C=C), 1246–1132 (C–N). <sup>1</sup>H NMR (300 Mhz, DMSO-d<sub>6</sub>, ppm)  $\delta$  0.92 (3H, d, *J* = 6.7 Hz, CH<sub>3</sub>), 1.04–1.13 (1H, m, piperidine-H), 1.50–1.79 (4H, m, piperidine-H), 2.39 (1H, t, *J* = 11.2 Hz, piperidine-H), 2.69 (1H, t, *J* = 12.2 Hz, piperidine-H), 3.68–3.75 (2H, m, piperidine-H), 6.96 (2H, d, *J* = 8.9 Hz, 1,4-disubstituted benzene), 7.42–7.47 (1H, m, quinoxaline), 7.57 (2H, d, *J* = 8.8 Hz, 1,4-disubstituted benzene), 7.63–7.65 (2H, m, quinoxaline), 7.88 (1H, d, *J* = 8.3 Hz, quinoxaline), 8.02 (1H, s, quinoxaline), 9.03 (1H, s, N=CH), 11.42 (1H, s, NH). <sup>13</sup>C NMR (75 MHz, DMSO-d<sub>6</sub>, ppm)  $\delta$  19.68 (CH<sub>3</sub>), 24.92, 30.56, 32.98, 48.46, 55.95, 115.26, 124.37, 125.11, 126.42, 128.20, 129.20, 130.66, 136.96, 138.14, 141.64, 143.08, 150.83, 152.19. HRMS (m/z): [M+H]<sup>+</sup> calcd for C<sub>21</sub>H<sub>23</sub>N<sub>5</sub>: 346.2026; found: 346.2011.

**2-[2-(4-(4-Methylpiperidin-1-yl)benzylidene)hydrazineyl]quinoxaline (5e)** Yield 65%, m.p. 232.5–234.2 °C. IR  $\nu_{\max}$  (cm<sup>-1</sup>): 3201 (N–H) 3089 (aromatic C–H), 2920 (aliphatic C–H), 1606–1492 (C=N, C=C), 1307–1093 (C–N). <sup>1</sup>H

NMR (300 Mhz, DMSO- $d_6$ , ppm)  $\delta$  0.93 (3H, d,  $J$  = 6.4 Hz, CH<sub>3</sub>), 1.13–1.26 (2H, m, piperidine-H), 1.49–1.57 (1H, m, piperidine-H), 1.69 (2H, d,  $J$  = 12.6 Hz, piperidine-H), 2.73 (1H, t,  $J$  = 12.4 Hz, piperidine-H), 3.79 (2H, d,  $J$  = 12.8 Hz, piperidine-H), 6.96 (2H, d,  $J$  = 8.9 Hz, 1,4-disubstituted benzene), 7.42–7.47 (1H, m, quinoxaline), 7.57 (2H, d,  $J$  = 9.0 Hz, 1,4-disubstituted benzene), 7.64–7.65 (2H, m, quinoxaline), 7.88 (1H, d,  $J$  = 8.1 Hz, quinoxaline), 8.02 (1H, s, quinoxaline), 9.03 (1H, s, N=CH), 11.42 (1H, s, NH). <sup>13</sup>C NMR (75 MHz, DMSO- $d_6$ , ppm)  $\delta$  22.23 (CH<sub>3</sub>), 30.71, 33.74, 48.40, 115.34, 124.48, 125.12, 126.43, 128.18, 129.20, 130.67, 136.96, 138.14, 141.63, 143.06, 150.83, 152.19. HRMS (m/z): [M+H]<sup>+</sup> calcd for C<sub>21</sub>H<sub>23</sub>N<sub>5</sub>: 346.2026; found: 346.2011.

**2-[2-(4-(3,5-Dimethylpiperidin-1-yl)benzylidene)hydrazineyl]quinoxaline (5f)** Yield 66%, m.p. 191.1–193.6 °C. IR  $\nu_{\max}$  (cm<sup>-1</sup>): 3201 (N–H) 3055 (aromatic C–H), 2989 (aliphatic C–H), 1614–1456 (C=N, C=C), 1342–1105 (C–N). <sup>1</sup>H NMR (300 Mhz, DMSO- $d_6$ , ppm)  $\delta$  0.66–0.78 (1H, m, piperidine-H), 0.93 (6H, d,  $J$  = 6.5 Hz, CH<sub>3</sub>), 1.61–1.78 (3H, m, piperidine-H), 2.25 (2H, t,  $J$  = 11.7 Hz, piperidine-H), 3.77 (2H, d,  $J$  = 12.3 Hz, piperidine-H), 6.96 (2H, d,  $J$  = 8.7 Hz, 1,4-disubstituted benzene), 7.42–7.47 (1H, m, quinoxaline), 7.56 (2H, d,  $J$  = 8.8 Hz, 1,4-disubstituted benzene), 7.63–7.65 (2H, m, quinoxaline), 7.88 (1H, d,  $J$  = 8.1 Hz, quinoxaline), 8.02 (1H, s, quinoxaline), 9.03 (1H, s, N=CH), 11.42 (1H, s, NH). <sup>13</sup>C NMR (75 MHz, DMSO- $d_6$ , ppm)  $\delta$  19.60 (CH<sub>3</sub>), 27.23, 30.50, 42.29, 55.45, 115.18, 124.25, 125.11, 126.42, 128.24, 129.20, 130.66, 136.95, 138.14, 141.64, 143.10, 150.83, 151.83. HRMS (m/z): [M+H]<sup>+</sup> calcd for C<sub>22</sub>H<sub>25</sub>N<sub>5</sub>: 360.2183; found: 360.2167.

**2-[2-(4-(4-Benzylpiperidin-1-yl)benzylidene)hydrazineyl]quinoxaline (5g)** Yield 78%, m.p. 248.9–251.1 °C. IR  $\nu_{\max}$  (cm<sup>-1</sup>): 3213 (N–H) 3082 (aromatic C–H), 2967 (aliphatic C–H), 1612–1492 (C=N, C=C), 1307–1099 (C–N). <sup>1</sup>H NMR (300 Mhz, DMSO- $d_6$ , ppm)  $\delta$  1.21–1.32 (2H, m, piperidine-H), 1.63–1.74 (3H, m, piperidine-H), 2.55 (2H, d,  $J$  = 7.0 Hz, CH<sub>2</sub>), 2.70 (2H, t,  $J$  = 12.4 Hz, piperidine-H), 3.80 (2H, d,  $J$  = 12.7 Hz, piperidine-H), 6.96 (2H, d,  $J$  = 8.8 Hz, 1,4-disubstituted benzene), 7.19–7.21 (3H, m, Monosubstituted benzene), 7.27–7.32 (2H, m, Monosubstituted benzene), 7.42–7.47 (1H, m, quinoxaline), 7.56 (2H, d,  $J$  = 8.9 Hz, 1,4-disubstituted benzene), 7.64–7.65 (2H, m, quinoxaline), 7.88 (1H, d,  $J$  = 8.2 Hz, quinoxaline), 8.02 (1H, s, quinoxaline), 9.02 (1H, s, N=CH), 11.42 (1H, s, NH). <sup>13</sup>C NMR (75 MHz, DMSO- $d_6$ , ppm)  $\delta$  31.58, 37.77, 42.70, 48.33, 115.36, 124.52, 125.13, 126.26, 126.43, 128.17, 128.62, 129.21, 129.49, 130.67, 136.95, 138.14, 140.65, 141.63, 143.03, 150.83, 152.14. HRMS (m/z): [M+H]<sup>+</sup> calcd for C<sub>27</sub>H<sub>27</sub>N<sub>5</sub>: 422.2339; found: 422.2321.

**2-[2-(4-(Morpholine-4-yl)benzylidene)hydrazineyl]quinoxaline (5h)** Yield 67%, m.p. 258.3–260.1 °C. IR  $\nu_{\max}$  (cm<sup>-1</sup>): 3207 (N–H) 3084 (aromatic C–H), 2993 (aliphatic C–H), 1612–1492 (C=N, C=C), 1309–1111 (C–N, C–O). <sup>1</sup>H NMR (300 Mhz, DMSO- $d_6$ , ppm)  $\delta$  3.20 (4H, t,  $J$  = 4.7 Hz, morpholine-H), 3.75 (4H, t,  $J$  = 5.0 Hz, morpholine-H), 7.00 (2H, d,  $J$  = 9.0 Hz, 1,4-disubstituted benzene), 7.43–7.48 (1H, m, quinoxaline), 7.60–7.65 (2H, m, quinoxaline), 7.89 (1H, d,  $J$  = 8.3 Hz, 1,4-disubstituted benzene), 8.05 (1H, s, quinoxaline), 9.04 (1H, s, N=CH), 11.47 (1H, s, NH). <sup>13</sup>C NMR (75 MHz, DMSO- $d_6$ , ppm)  $\delta$  48.12, 66.45, 115.02, 125.20, 125.61, 126.46, 128.11, 129.21, 130.69, 136.96, 138.18, 141.60, 142.84, 150.83, 152.14. HRMS (m/z): [M+H]<sup>+</sup> calcd for C<sub>19</sub>H<sub>19</sub>N<sub>5</sub>O: 334.1662; found: 334.1646.

**2-[2-(4-(4-Methylpiperazin-1-yl)benzylidene)hydrazineyl]quinoxaline (5i)** Yield 60%, m.p. 221.9–224.3 °C. IR  $\nu_{\max}$  (cm<sup>-1</sup>): 3207 (N–H) 3057 (aromatic C–H), 2926 (aliphatic C–H), 1577–1481 (C=N, C=C), 1246–1132 (C–N). <sup>1</sup>H NMR (300 Mhz, DMSO- $d_6$ , ppm)  $\delta$  2.22 (3H, s, CH<sub>3</sub>), 2.45 (4H, t,  $J$  = 4.9 Hz, piperazine-H), 3.23 (4H, t,  $J$  = 4.7 Hz, piperazine-H), 6.98 (2H, d,  $J$  = 8.9 Hz, 1,4-disubstituted benzene), 7.42–7.48 (1H, m, quinoxaline), 7.59 (2H, d,  $J$  = 8.9 Hz, 1,4-disubstituted benzene), 7.64–7.65 (2H, m, quinoxaline), 7.88 (1H, d,  $J$  = 8.1 Hz, quinoxaline), 8.03 (1H, s, quinoxaline), 9.04 (1H, s, N=CH), 11.45 (1H, s, NH). <sup>13</sup>C NMR (75 MHz, DMSO- $d_6$ , ppm)  $\delta$  46.21 (CH<sub>3</sub>), 47.74, 54.91, 115.18, 125.14, 125.17, 126.43, 128.11, 129.21, 130.68, 136.97, 138.16, 141.60, 142.94, 150.82, 152.04. HRMS (m/z): [M+H]<sup>+</sup> calcd for C<sub>20</sub>H<sub>22</sub>N<sub>6</sub>: 347.1979; found: 347.1973.

**2-[2-(4-(4-Ethylpiperazin-1-yl)benzylidene)hydrazineyl]quinoxaline (5j)** Yield 69%, m.p. 212.0–213.9 °C. IR  $\nu_{\max}$  (cm<sup>-1</sup>): 3167 (N–H) 3057 (aromatic C–H), 2967 (aliphatic C–H), 1612–1489 (C=N, C=C), 1244–1128 (C–N). <sup>1</sup>H NMR (300 Mhz, DMSO- $d_6$ , ppm)  $\delta$  1.02 (3H, t,  $J$  = 7.1 Hz, CH<sub>3</sub>), 2.35 (2H, q,  $J$  = 7.2 Hz, CH<sub>2</sub>), 2.46–2.49 (4H, m, piperazine-H), 3.21 (4H, t,  $J$  = 4.9 Hz, piperazine-H), 6.97 (2H, d,  $J$  = 8.7 Hz, 1,4-disubstituted benzene), 7.42–7.47 (1H, m, quinoxaline), 7.59 (2H, d,  $J$  = 8.7 Hz, 1,4-disubstituted benzene), 7.64–7.65 (2H, m, quinoxaline), 7.88 (1H, d,  $J$  = 8.1 Hz, quinoxaline), 8.03 (1H, s, quinoxaline), 9.04 (1H, s, N=CH), 11.46 (1H, s, NH). <sup>13</sup>C NMR (75 MHz, DMSO- $d_6$ , ppm)  $\delta$  12.44 (CH<sub>3</sub>), 47.86 (CH<sub>2</sub>), 52.08, 52.67, 115.12, 125.11, 125.16, 126.43, 128.10, 129.21, 130.67, 136.96, 138.16, 141.61, 142.94, 150.83, 152.07. HRMS (m/z): [M+H]<sup>+</sup> calcd for C<sub>21</sub>H<sub>24</sub>N<sub>6</sub>: 361.2135; found: 361.2122.

**2-[2-[4-(4-(4-Methoxyphenyl)piperazin-1-yl)benzylidene]hydrazineyl]quinoxaline (5k)** Yield 65%, m.p. 260.8–263.1 °C. IR  $\nu_{\max}$  (cm<sup>-1</sup>): 3196 (N–H) 3062 (aromatic C–H), 2956 (aliphatic C–H), 1606–1510 (C=N, N–O).

C=C), 1296–1020 (C–N, C–O).  $^1\text{H}$  NMR (300 Mhz, DMSO- $d_6$ , ppm)  $\delta$  3.16 (4H, t,  $J = 5.0$  Hz, piperazine-H), 3.38 (4H, t,  $J = 4.1$  Hz, piperazine-H), 3.69 (3H, s, OCH<sub>3</sub>), 6.84 (2H, d,  $J = 9.0$  Hz, 1,4-disubstituted benzene), 6.96 (2H, d,  $J = 9.0$  Hz, 1,4-disubstituted benzene), 7.05 (2H, d,  $J = 8.9$  Hz, 1,4-disubstituted benzene), 7.43–7.48 (1H, m, quinoxaline), 7.61–7.66 (4H, m, 1,4-disubstituted benzene, quinoxaline), 7.89 (1H, d,  $J = 8.1$  Hz, quinoxaline), 8.05 (1H, s, quinoxaline), 9.05 (1H, s, N=CH), 11.47 (1H, s, NH).  $^{13}\text{C}$  NMR (75 MHz, DMSO- $d_6$ , ppm)  $\delta$  48.09, 50.15, 55.65, 114.77, 115.46, 118.22, 125.20, 125.45, 126.46, 128.16, 129.22, 130.70, 136.98, 138.18, 141.61, 142.88, 145.70, 150.83, 151.97, 153.66. HRMS (m/z): [M+H]<sup>+</sup> calcd for C<sub>26</sub>H<sub>26</sub>N<sub>6</sub>O: 439.2241; found: 439.2234.

**2-[2-[4-(4-(2-(N,N-Dimethylamino)ethyl)piperazin-1-yl)benzylidene]hydrazineyl] quinoxaline (5l):** Yield 64%, m.p. 190.3–192.2 °C. IR  $\nu_{\text{max}}$  (cm<sup>-1</sup>): 3201 (N–H) 3053 (aromatic C–H), 2954 (aliphatic C–H), 1608–1492 (C=N, C=C), 1305–1107 (C–N).  $^1\text{H}$  NMR (300 Mhz, DMSO- $d_6$ , ppm)  $\delta$  2.14 (6H, s, 2CH<sub>3</sub>), 2.32–2.44 (4H, m, CH<sub>2</sub>–CH<sub>2</sub>), 2.51–2.53 (4H, m, piperazine-H), 3.20 (4H, t,  $J = 4.2$  Hz, CH<sub>3</sub>), 6.96 (2H, d,  $J = 8.9$  Hz, 1,4-disubstituted benzene), 7.42–7.47 (1H, m, quinoxaline), 7.58 (2H, d,  $J = 8.6$  Hz, 1,4-disubstituted benzene), 7.64–7.65 (2H, m, quinoxaline), 7.88 (1H, d,  $J = 8.3$  Hz, quinoxaline), 8.03 (1H, s, quinoxaline), 9.04 (1H, s, N=CH), 11.46 (1H, s, NH).  $^{13}\text{C}$  NMR (75 MHz, DMSO- $d_6$ , ppm)  $\delta$  46.01, 47.88, 53.40, 56.30, 57.11, 115.12, 125.13, 126.43, 128.10, 129.21, 130.67, 136.96, 138.16, 141.61, 142.93, 150.83, 152.05. HRMS (m/z): [M+H]<sup>+</sup> calcd for C<sub>23</sub>H<sub>29</sub>N<sub>7</sub>: 404.2557; found: 404.2541.

**2-[2-[4-(4-(3-(N,N-Dimethylamino)propyl)piperazin-1-yl)benzylidene]hydrazineyl] quinoxaline (5m):** Yield 72%, m.p. 194.8–196.9 °C. IR  $\nu_{\text{max}}$  (cm<sup>-1</sup>): 3201 (N–H) 3053 (aromatic C–H), 2941 (aliphatic C–H), 1610–1492 (C=N, C=C), 1228–1107 (C–N).  $^1\text{H}$  NMR (300 Mhz, DMSO- $d_6$ , ppm)  $\delta$  1.57 (2H, p,  $J = 7.1$  Hz, CH<sub>2</sub>–CH<sub>2</sub>–CH<sub>2</sub>), 2.11 (6H, s, 2CH<sub>3</sub>), 2.21 (2H, t,  $J = 7.5$  Hz, CH<sub>2</sub>), 2.32 (2H, t,  $J = 7.5$  Hz, CH<sub>2</sub>), 2.47 (4H, t,  $J = 4.9$  Hz, piperazine-H), 3.22 (4H, t,  $J = 4.9$  Hz, piperazine-H), 6.97 (2H, d,  $J = 8.9$  Hz, 1,4-disubstituted benzene), 7.43–7.48 (1H, m, quinoxaline), 7.59 (2H, d,  $J = 8.7$  Hz, 1,4-disubstituted benzene), 7.64–7.65 (2H, m, quinoxaline), 7.88 (1H, d,  $J = 8.1$  Hz, quinoxaline), 8.03 (1H, s, quinoxaline), 9.04 (1H, s, N=CH), 11.47 (1H, s, NH).  $^{13}\text{C}$  NMR (75 MHz, DMSO- $d_6$ , ppm)  $\delta$  24.99, 45.71, 47.89, 53.14, 56.50, 57.78, 115.14, 125.12, 125.16, 126.43, 128.11, 129.21, 130.68, 136.97, 138.15, 141.61, 142.95, 150.83, 152.07. HRMS (m/z): [M+H]<sup>+</sup> calcd for C<sub>24</sub>H<sub>31</sub>N<sub>7</sub>: 418.2714; found: 418.2695.

## Activity studies

### Monoamine oxidase activity assay

The inhibitory activities of the obtained compounds against MAO-A and MAO-B enzymes were evaluated in black bottom 96-well plates by method as defined in our previous studies (Can et al. 2017, 2018). All pipetting procedures in the enzyme inhibition assay were carried out using a robotic system, Biotek Precision XS (Winooski, VT, USA). Selegiline and chlorgiline were used as reference drugs. The IC<sub>50</sub> values were calculated from a dose-response curve gained by plotting the percentage inhibition versus the log concentration with the use of GraphPad PRISM software (version 5.0, GraphPad Software Inc., La Jolla, CA, USA). The results are showed as the mean  $\pm$  standard deviation.

The inhibitory capacity of the obtained compounds on AChE and BChE biological activities was assessed using a modified Ellman's spectrometric method, as described in our previous studies (Acar Çevik et al. 2019; Özkay et al. 2016; Sağlık et al. 2016; Hussein et al. 2018; Tok et al. 2019). Donepezil was used as a reference drug. All pipetting procedures in the enzyme inhibition assay were carried out via a robotics system, Biotek Precision XS (Winooski, VT, USA). A BioTek-Synergy H1 microplate reader (Winooski, VT, USA) was used to carry out measurements of percent inhibition at 412 nm, and the IC<sub>50</sub> values of the selected compounds were performed as previously described.

### Molecular docking studies

Molecular docking studies were performed to discover the binding modes of compound 5l to active sites of AChE and MAO-B enzymes, respectively. The crystal structures of AChE (PDB code: 4EY7) (Cheung et al. 2012) and MAO-B (PDB code: 2V5Z) (Claudia et al. 2007) were retrieved from the Protein Data Bank server ([www.pdb.org](http://www.pdb.org)). Docking procedures were followed as reported previously (Tok et al. 2019; Sağlık et al. 2016; Kaya Çavuşoğlu et al. 2018a, 2018b; Can et al. 2017; Sağlık et al. 2019).

## Results and discussion

### Chemistry

Target compounds (5a–5m) were efficiently synthesized according to the protocol outlined in Scheme 1. The chemical structure of the compounds is organized in Table 1. Following the microwave supported synthesis of quinoxaline-2(1H)-one (1), 2-chloroquinoxaline (2) was synthesized

**Scheme 1** The reaction sequence for the synthesis of the compounds (**5a–5m**). Reagents and conditions: (i) EtOH, MW, 200 °C, 25 bar, 15 min; (ii) POCl<sub>3</sub>, reflux, 3 h; (iii) NH<sub>2</sub>NH<sub>2</sub>·H<sub>2</sub>O, THF, MW, 10 bar, 170 °C, 15 min; (iv) DMF, K<sub>2</sub>CO<sub>3</sub>, reflux, 24 h; (v) CH<sub>3</sub>COOH, EtOH, reflux, 1 h

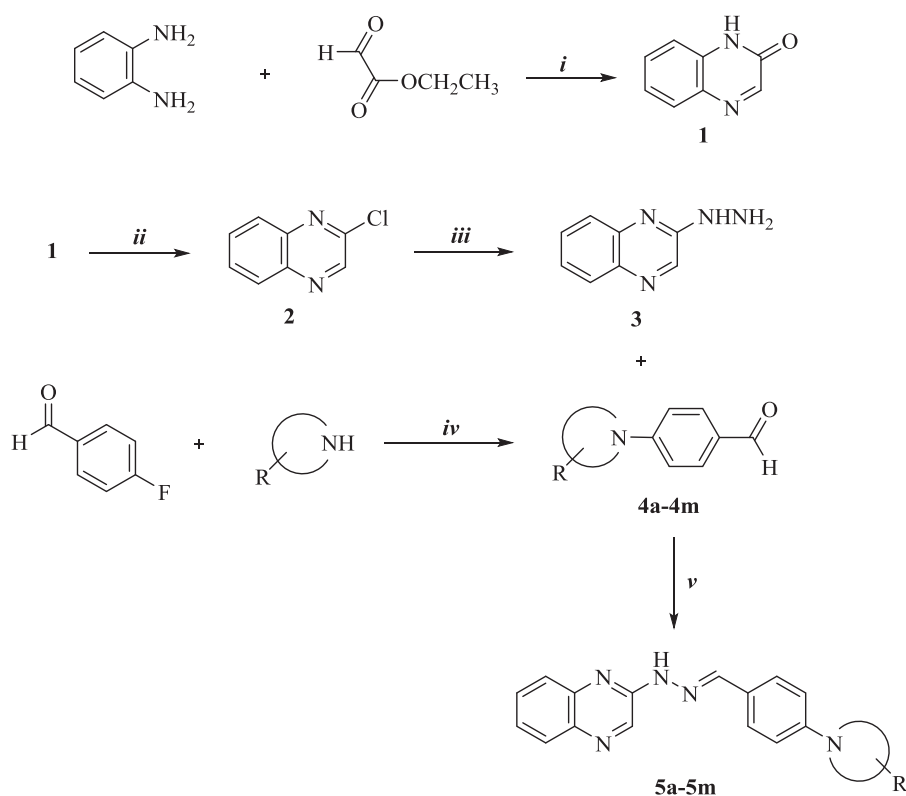


**Table 1** The synthesized compounds (**5a–5m**)

Compound	Secunder amine
<b>5a</b>	pyrrolidine
<b>5b</b>	piperidine
<b>5c</b>	2-metilpiperidine
<b>5d</b>	3-metilpiperidine
<b>5e</b>	4-metilpiperidine
<b>5f</b>	3,5-dimetilpiperidine
<b>5g</b>	4-benzylpiperidine
<b>5h</b>	morpholine
<b>5i</b>	4-metilpiperazine
<b>5j</b>	4-ethylpiperazine
<b>5k</b>	4-(4-metoxifenil)piperazine
<b>5l</b>	4-(dimetilaminoetil)piperazine
<b>5m</b>	4-(dimetilaminopropil)piperazine

via the reaction of compound **1** and phosphoryl chloride. The intermediate compound **2** was reacted hydrazine hydrate to gain quinoxaline-2-hydrazine (**3**). In order to obtain several benzaldehyde derivatives (**4a–4m**), appropriate secunder amines and 4-fluorophenylbenzaldehyde were refluxed in dimethylformamide. Finally, the treatment of quinoxaline-2-hydrazine (**3**) with the synthesized benzaldehyde derivatives (**4a–4m**) in ethanol with catalytic

amount of acetic acid gave the designed compounds (**5a–5m**).

The IR, <sup>1</sup>H NMR, <sup>13</sup>C NMR and MS spectral data of the compounds provided evidence for the formation of the expected structures. In the IR spectra of all compounds, Broad peaks at 3150–3370 cm<sup>-1</sup> indicated N–H stretching vibrations of hydrazine. The C=N and C=C stretching vibration bands were observed in the expected region: 1630–1667 cm<sup>-1</sup>. In <sup>1</sup>H NMR spectrum of compounds, protons belonging to pyrrolidine, piperidine, piperazine, and morpholine rings resonated at 0.66–4.21 ppm. The azomethine (N=CH) protons of hydrazone were observed at 9.02–9.05 ppm as a singlet. The protons belonging to the phenyl and quinoxaline rings and the other aliphatic groups were observed with the expected chemical shift and integral values. The NH protons were appeared at 11.42–11.47 ppm as singlet peak. In <sup>13</sup>C NMR spectra of compounds, aromatic carbons were resonated a large area between 114.77–153.66 ppm. The mass spectra of compounds showed [M + 1] peaks, in agreement with their molecular formula.

### Monoamine oxidase activity assay

The synthesized compounds were evaluated for their *h*MAO-A and *h*MAO-B inhibitory activities. In addition, selegiline and moclobemide were evaluated as reference

**Table 2** % Inhibition of compounds **5a–5m**, moclobemide and selegiline against *h*MAO-A and *h*MAO-B

Comp.	<i>h</i> MAO-A inhibition %		<i>h</i> MAO-B inhibition %	
	$10^{-3}$ M	$10^{-4}$ M	$10^{-3}$ M	$10^{-4}$ M
<b>5a</b>	77.798 ± 1.252	49.020 ± 0.833	98.338 ± 1.467	94.226 ± 1.108
<b>5b</b>	72.068 ± 1.329	48.460 ± 0.604	98.826 ± 1.244	96.240 ± 1.066
<b>5c</b>	82.554 ± 1.096	23.359 ± 0.708	94.216 ± 1.538	39.846 ± 0.632
<b>5d</b>	85.454 ± 1.136	48.016 ± 0.539	52.528 ± 0.875	48.586 ± 0.611
<b>5e</b>	83.816 ± 1.018	37.405 ± 0.647	93.138 ± 1.148	44.473 ± 0.975
<b>5f</b>	82.443 ± 1.114	47.786 ± 0.788	94.516 ± 1.007	89.326 ± 1.106
<b>5g</b>	49.619 ± 0.992	36.800 ± 0.851	75.150 ± 0.877	41.902 ± 0.319
<b>Moclobemide</b>	94.125 ± 2.760	82.143 ± 2.694	–	–
<b>5h</b>	81.170 ± 1.007	39.847 ± 0.631	76.864 ± 1.028	45.501 ± 0.871
<b>5i</b>	60.153 ± 1.066	20.695 ± 0.475	83.676 ± 1.244	46.015 ± 0.905
<b>5j</b>	58.168 ± 0.952	22.137 ± 0.455	69.152 ± 0.955	38.303 ± 0.417
<b>5k</b>	53.893 ± 0.962	34.952 ± 0.671	66.581 ± 0.819	20.280 ± 0.332
<b>5l</b>	54.504 ± 0.976	29.313 ± 0.411	99.531 ± 1.116	95.631 ± 1.085
<b>5m</b>	48.050 ± 0.823	26.209 ± 0.529	87.295 ± 1.259	48.806 ± 0.511
<b>Selegiline</b>	–	–	98.912 ± 1.281	96.882 ± 1.313

compounds. The results, expressed as % inhibition and  $IC_{50}$  values are summarized in Tables 2 and 3. In the first step, the synthesized compounds were prepared at concentrations of  $10^{-3}$  ve  $10^{-4}$  M and inhibition values of *h*MAO A and *h*MAO B were calculated. The compounds showing >50% inhibition were selected for the second stage according to the first step results. In this second step, inhibition values and  $IC_{50}$  values of the selected compounds at concentrations of  $10^{-5}$ – $10^{-9}$  M were calculated. Considering Table 2, only compound **5l** passed the second step *h*MAO-B enzyme inhibition assay.

Generally, the compounds showed higher activity against *h*MAO-B than *h*MAO-A. In particular compound **5l** has a significant activity value against *h*MAO-B. Compound **5l** efficient inhibition against *h*MAO-B with  $IC_{50}$  value of  $0.046 \pm 0.002$   $\mu$ M. Compared with the reference drug selegiline, it is clear that it shows significant activity.

### Anticholinesterase activity assay

To determine the potential interest of the quinoxaline-hydrazone synthesized, AChE and BChE inhibitory potency was assessed according to modified Ellman method with commercially obtainable donepezil as the reference standard. Initially, all the obtained compounds were tested at  $10^{-3}$  M and  $10^{-4}$  M concentrations and The ChE inhibitory results are outlined in Table 4. With respect to the activity results, it was determined that most of the tested compounds showed better inhibitory activity against AChE than BChE activity. Compound **5l** indicated more than 50% activity at

**Table 3**  $IC_{50}$  values of compounds **5a**, **5b**, **5f**, **5l** and selegiline against MAO-B

Compound	<i>h</i> MAO-B $IC_{50}$ ( $\mu$ M)
<b>5a</b>	$0.098 \pm 0.003$
<b>5b</b>	$0.075 \pm 0.002$
<b>5f</b>	$0.113 \pm 0.004$
<b>5l</b>	$0.046 \pm 0.002$
<b>Selegiline</b>	$0.039 \pm 0.001$

the  $10^{-4}$  M concentration. Then, the  $IC_{50}$  values of the active compounds were determined using  $10^{-3}$ – $10^{-9}$  M concentrations against AChE along with the reference drug donepezil (Table 5). The  $IC_{50}$  values of the compound **5l** were calculated as  $0.028 \pm 0.001$   $\mu$ M for AChE. Compared with the reference drug, it is clear that it shows similar activity with donepezil.

### Molecular docking studies

Docking studies were performed in order to gain more insight into the binding modes of compound **5l** to AChE and MAO-B enzymes. Studies were carried out by using the X-ray crystal structures of *Homo sapiens* AChE (hAChE PDB ID:4EY7) (Cheung et al. 2012) and MAO-B (PDB ID: 2V5Z) (Claudia et al. 2007) obtained from Protein Data Bank server ([www.pdb.org](http://www.pdb.org)).

**Table 4** % Inhibition of compounds **5a–5m**, donepezil and tacrine against AChE and BChE

Comp.	AChE inhibition %		BChE inhibition %	
	$10^{-3}$ M	$10^{-4}$ M	$10^{-3}$ M	$10^{-4}$ M
<b>5a</b>	55.411 ± 0.994	48.165 ± 0.754	39.921 ± 0.898	30.456 ± 0.641
<b>5b</b>	58.837 ± 0.905	42.629 ± 0.623	28.078 ± 0.545	21.826 ± 0.711
<b>5c</b>	49.550 ± 0.529	41.307 ± 0.872	34.512 ± 0.806	27.146 ± 0.455
<b>5d</b>	47.007 ± 0.808	38.824 ± 0.621	42.926 ± 0.623	30.674 ± 0.477
<b>5e</b>	42.678 ± 0.429	36.458 ± 0.337	38.306 ± 0.629	31.134 ± 0.558
<b>5f</b>	53.178 ± 0.994	47.869 ± 0.420	29.835 ± 0.599	20.660 ± 0.318
<b>5g</b>	39.618 ± 0.825	33.460 ± 0.525	33.431 ± 0.488	30.167 ± 0.320
<b>Donepezil</b>	99.258 ± 1.168	98.542 ± 1.095	–	–
<b>5h</b>	41.362 ± 0.318	35.060 ± 0.479	38.658 ± 0.759	27.507 ± 0.605
<b>5i</b>	95.280 ± 1.299	88.256 ± 1.011	44.396 ± 0.298	36.125 ± 0.355
<b>5j</b>	96.750 ± 1.106	85.248 ± 1.126	29.893 ± 0.411	22.627 ± 0.359
<b>5k</b>	68.871 ± 1.062	44.674 ± 0.718	35.346 ± 0.782	31.104 ± 0.699
<b>5l</b>	99.625 ± 1.297	97.662 ± 1.268	48.067 ± 0.520	30.020 ± 0.498
<b>5m</b>	98.147 ± 1.062	95.336 ± 1.108	36.869 ± 0.525	31.661 ± 0.417
<b>Tacrine</b>	–	–	98.248 ± 1.019	96.275 ± 1.471

The docking poses of compound **5l** for AChE enzyme are presented in Figs 2 and 3. According to these poses, it is clearly understood that compound **5l** binds to AChE enzyme in a similar position with donepezil due to the dual binding sites. The quinoxaline ring of compound forms the lipophilic part, whereas the polar basic center is consisted of dimethylaminoethylpiperazine moiety. The docking poses specify that lipophilic group of the structure bind to PAS region of AChE, while CAS region of the enzyme interacts with the polar basic center.

It is observed that the quinoxaline ring is in interaction with indole of Trp286 by  $\pi$ - $\pi$  interaction. Other  $\pi$ - $\pi$  interactions are identified between the phenyl ring in the middle of the structure and phenyl rings of Phe338 and Tyr341. Also, hydrazone moiety of the structure is essential for polar interactions. Amine moiety of hydrazone group interacts with carbonyl of Arg296 by forming a hydrogen bond. Another hydrogen bond is related to nitrogen of imine group. The nitrogen atom of imine forms a hydrogen bond with amino of Phe295. An efficient binding is also provided by the formation of cation- $\pi$  interaction between the nitrogen atom of dimethylaminoalkyl group and indole of Trp86. Furthermore, this nitrogen atom creates salt bridge with Glu202. Docking results also show that extended carbon chain enhances the van der Waals interactions with the amino acids in the active site and intensifies the proper bonding.

Three-dimensional poses of compound **5l** in the active site of MAO-B are presented in Figs 4 and 5. The compound **5l** adequately binds to amino acid residues, lining the cavity by overlapping at the same site and, locating very

**Table 5** IC<sub>50</sub> values of compounds **5i**, **5j**, **5l**, **5m** and donepezil against AChE

Compound	AChE IC <sub>50</sub> (μM)
<b>5i</b>	0.106 ± 0.003
<b>5j</b>	0.187 ± 0.007
<b>5l</b>	0.028 ± 0.001
<b>5m</b>	0.042 ± 0.002
<b>Donepezil</b>	0.026 ± 0.001

near the FAD cofactor. According to docking poses, the quinoxaline ring creates a  $\pi$ - $\pi$  interaction with phenyl of Tyr435. There is another  $\pi$ - $\pi$  interaction between phenyl ring near to piperazine and phenyl of Tyr326. The amine group of hydrazone moiety in the structure interacts with carbonyl of Glu206 by the formation of a hydrogen bond. Another hydrogen bond is observed between the nitrogen atom of dimethylaminoalkyl chain and carbonyl of Pro102. It is thought that this interaction is answer to why compound **5l** is the most active derivative in the series.

## Conclusion

To develop biologically active derivatives, the presence of a pharmacophore group in the compounds that synthesis is planned is a basic approach in pharmaceutical chemistry. Based on this approach, quinoxaline and hydrazone in



**Fig. 2** Three-dimensional pose of compound **51** (orange colored) in the enzyme active site (AChE PDB Code: 4EY7)

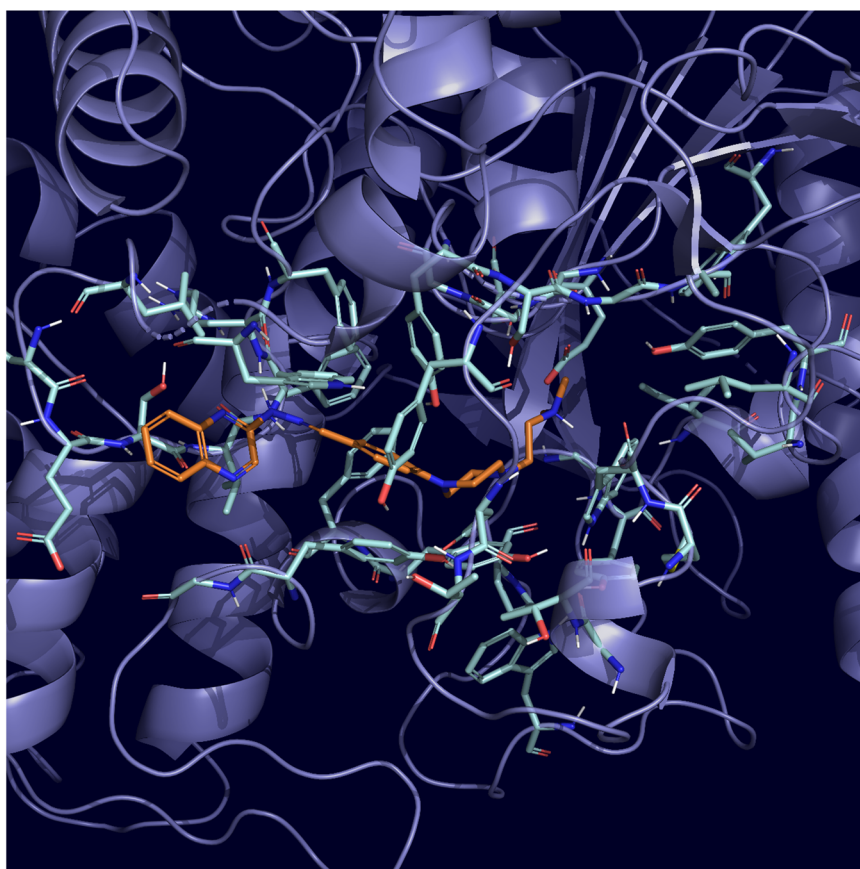
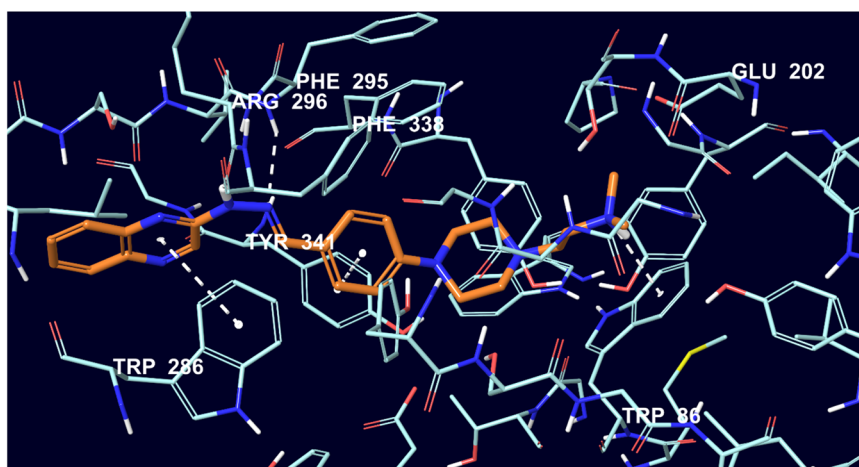


**Fig. 3** The interacting mode of compound **51** in the active region of AChE. The inhibitor, colored with orange, and the important residues, colored with turquoise, in the active site of the enzyme are presented by tube model



which we reported MAO and ChE inhibitor activities in previous studies were combined at the same molecule. MAO and ChE inhibitor activities of the obtained compounds were performed. Generally obtained compounds showed more activity against *h*MAO-B and AChE enzymes. According to the results of the *in vitro* MAO and

ChE enzyme inhibition assay, it was found that the compound **51** is the most active derivative against both enzymes. Compound **51** bearing dimethylaminoethyl moiety is similar acetylcholine molecule. High activity in this compound suggests that it acts as acetylcholine and inhibits the enzyme.

**Fig. 4** Three-dimensional pose of compound **51** in the enzyme active site (MAO-B PDB Code: 2V5Z)

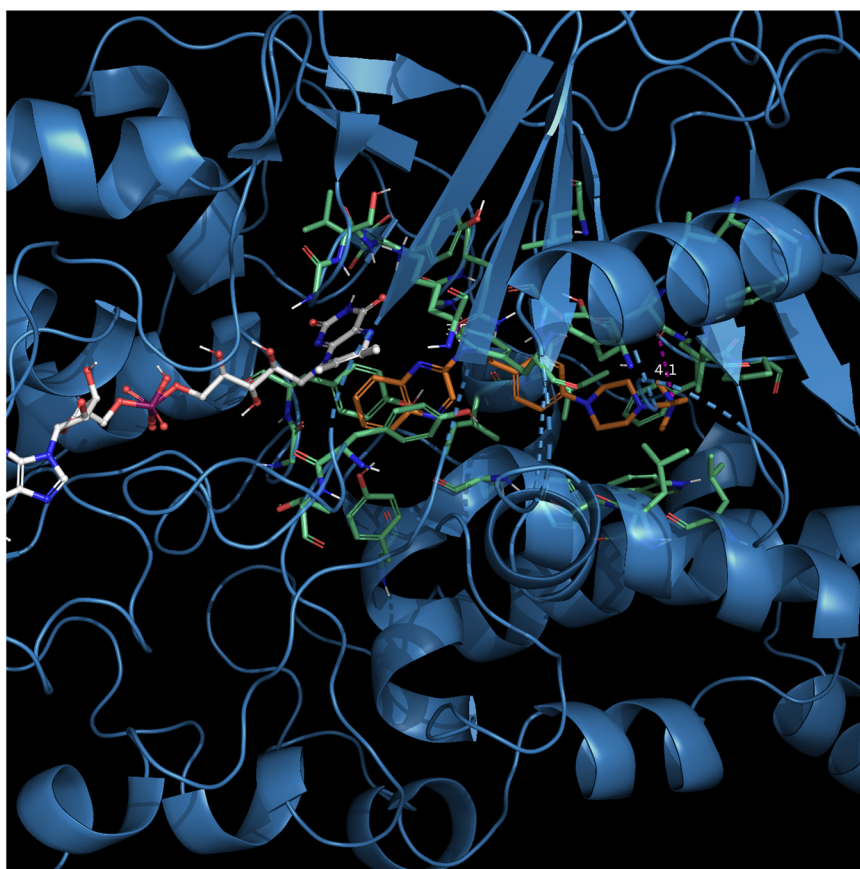
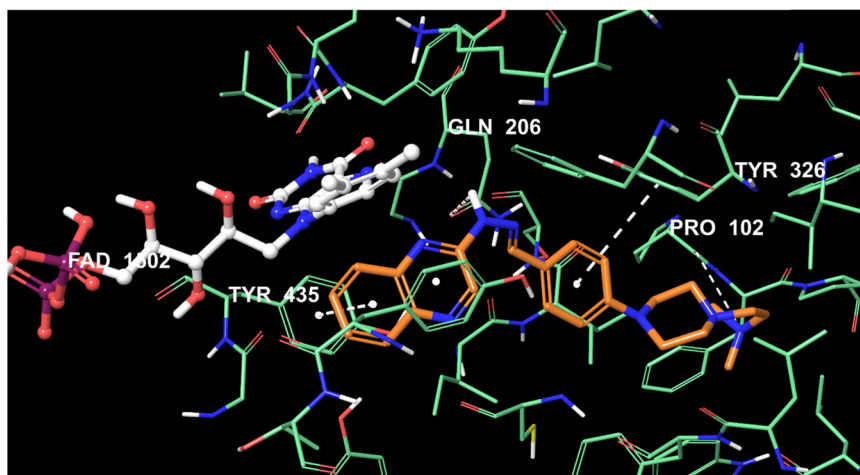


**Fig. 5** The interacting mode of compound **51** in the active region of MAO-B. The inhibitor and the important residues in the active site of the enzyme are presented by tube model. The inhibitor is colored with orange. The FAD molecule is colored white with ball and stick model



**Acknowledgements** This study was financially supported by Anadolu University Scientific Projects Fund, Project No: 1805S190 and 1905S033.

### Compliance with ethical standards

**Conflict of interest** The authors declare that they have no conflict of interest.

**Publisher's note** Springer Nature remains neutral with regard to jurisdictional claims in published maps and institutional affiliations.

### References

Acar Çevik U, Sağlık BN, Levent S, Osmaniye D, Kaya Çavuşoğlu B, Özkay Y, Kaplancıklı ZA (2019) Synthesis and AChE-inhibitory activity of new benzimidazole derivatives. *Molecules* 24(5):861

- Bar-Am O, Amit T, Weinreb O, Youdim MB, Mandel S (2010) Propargylamine containing compounds as modulators of proteolytic cleavage of amyloid-beta protein precursor: involvement of MAPK and PKC activation. *J Alzheimer's Dis* 21(2):361–371
- Becker I (2008) Preparation of derivatives of 1-(2-pyrimidinyl) piperazine as potential anti-anxiety, antidepressant, and anti-psychotic agents. *J Het Chem* 45:1005–1022
- Can ÖD, Osmaniye D, Demir Özkay Ü, Sağlık BN, Levent S, İlgin S, Baysal M, Özkay Y, Kaplancıklı ZA (2017) MAO enzymes inhibitory activity of new benzimidazole derivatives including hydrazone and propargyl side chains. *Eur J Med Chem* 131:92–106
- Can NÖ, Osmaniye D, Levent S, Sağlık BN, Korkut B, Atlı Ö, Özkay Y, Kaplancıklı ZA (2018) Design, synthesis and biological assessment of new thiazolylhydrazone derivatives as selective and reversible hMAO-A inhibitors. *Eur J Med Chem* 144:68–81
- Chen CY, Lin TP, Chen CK, Lin SC, Tseng MS, Wen YS, Sun SS (2008) New chromogenic and fluorescent probes for anion detection: formation of a [2+2] supramolecular complex on addition of fluoride with positive homotropic cooperativity. *J Org Chem* 73(3):900–911
- Cheung J, Rudolph MJ, Burshteyn F, Cassidy MS, Gary EN, Love J, Matthew CF, Height JJ (2012) Structures of human acetylcholinesterase in complex with pharmacologically important ligands. *J Med Chem* 55:10282–10286
- Claudia B, Wang J, Pisani L, Caccia C, Carotti A, Salvati P, Edmondson DE, Mattevi A (2007) Structures of human monoamine oxidase B complexes with selective noncovalent inhibitors: safinamide and coumarin analogs. *J Med Chem* 50:5848–5852
- D'Ascenzio M, Chimenti P, Gidaro MC, De Monte C, De Vita D, Granese A, Scipione L, Di Santo R, Costa G, Alcaro S, Yáñez M, Carradori S (2015) (Thiazol-2-yl)hydrazone derivatives from acetylpyridines as dual inhibitors of MAO and AChE: synthesis, biological evaluation and molecular modeling studies. *J Enzyme Inhib Med Chem* 30(6):908–919
- Dias Viegas FP, de Freitas Silva M, Divino da Rocha M, Castelli MR, Riquiel MM, Machado RP, Vaz SM, Simões de Lima LM, Mancini KC, Marques de Oliveira PC, Morais ÉP, Gontijo VS, da Silva FMR, D'Alincourt da Fonseca Peçanha D, Castro NG, Neves GA, Giusti-Paiva A, Vilela FC, Orlandi L, Camps I, Veloso MP, Leomil Coelho LF, Ionta M, Ferreira-Silva GA, Pereira RM, Dardenne LE, Guedes IA, de Oliveira Carneiro Jr W, Quaglio Bellozi PM, Pinheiro de Oliveira AC, Ferreira FF, Pruccoli L, Tarozzi A, Viegas C (2018) Design, synthesis and pharmacological evaluation of N-benzyl-piperidinyl-aryl-acetylhydrazone derivatives as donepezil hybrids: discovery of novel multi-target anti-alzheimer prototype drug candidates. *Eur J Med Chem* 147:48–65
- Edmondson DE, Mattevi A, Binda C, Li M, Hubálek F (2004) Structure and mechanism of monoamine oxidase. *Curr Med Chem* 11:1983–1993
- Evranos-Aksöz B, Baysal İ, Yabanoğlu-Çiftçi S, Djikic T, Yelekçi K, Uçar G, Ertan R (2015) Synthesis and screening of human monoamine oxidase-A inhibitor effect of new 2-pyrazoline and hydrazone derivatives. *Arch Pharm Chem Life Sci* 348(10):743–756
- Huang W, Tang L, Shi Y, Huang S, Xu L, Sheng R, Wu P, Li J, Zhou N, Hu Y (2011) Searching for the Multi-Target-Directed Ligands against Alzheimer's disease: discovery of quinoxaline-based hybrid compounds with AChE, H3R and BACE 1 inhibitory activities. *Bioorg Med Chem* 19(23):7158–7167
- Hussein W, Sağlık BN, Levent S, Korkut B, İlgin S, Özkay Y, Kaplancıklı ZA (2018) Synthesis and biological evaluation of new cholinesterase inhibitors for Alzheimer's disease. *Molecules* 23:2033
- Karaman N, Sıcak Y, Taşkın-Tok T, Öztürk M, Karaküçük-İyidoğan A, Dikmen M, Koçyiğit-Kaymakçioğlu B, Oruç-Emre EE (2016) New piperidine-hydrazone derivatives: synthesis, biological evaluations and molecular docking studies as AChE and BChE inhibitors. *Eur J Med Chem* 124:270–283
- Kaya Çavuşoğlu B, Sağlık BN, Osmaniye D, Levent S, Acar Çevik U, Karaduman A, Özkay Y, Kaplancıklı Z (2018a) Synthesis and biological evaluation of new thiosemicarbazone derivative Schiff bases as monoamine oxidase inhibitory agents. *Molecules* 23:60
- Kaya Çavuşoğlu B, Sağlık BN, Özkay Y, İnci B, Kaplancıklı ZA (2018b) Design, synthesis, monoamine oxidase inhibition and docking studies of new dithiocarbamate derivatives bearing benzylamine moiety. *Bioorg Chem* 76:177–187
- Khatab SN, Abdel Moneim SA, Bekhit AA, El Massry AM, Hassan SY, El-Faham A, Ali Ahmed HE, Amer A (2015) Exploring new selective 3-benzylquinoxaline-based MAO-A inhibitors: design, synthesis, biological evaluation and docking studies. *Eur J Med Chem* 93:308–320
- Khatab SN, Hassan SY, Bekhit AA, El Massry AM, Langer V, Amer A (2010) Synthesis of new series of quinoxaline based MAO-inhibitors and docking studies. *Eur J Med Chem* 45(10):4479–4489
- Li Y, Qiang X, Luo L, Yang X, Xiao G, Zheng Y, Cao Z, Sang Z, Su F, Deng Y (2017) Multitarget drug design strategy against Alzheimer's disease: homoisoflavonoid Mannich base derivatives serve as acetylcholinesterase and monoamine oxidase B dual inhibitors with multifunctional properties. *Bioorg Med Chem* 25(2):714–726
- Osmaniye D, Sağlık BN, Acar Çevik U, Levent S, Kaya Çavuşoğlu B, Özkay Y, Kaplancıklı ZA, Turan G (2019) Synthesis and AChE inhibitory activity of novel thiazolylhydrazone derivatives. *Molecules* 24(13):2392
- Özkay ÜD, Can ÖD, Sağlık BN, Çevik UA, Levent S, Özkay Y, İlgin S, Atlı Ö (2016) Design, synthesis, and AChE inhibitory activity of new benzothiazole-piperazines. *Bioorg Med Chem Lett* 26:5387–5394
- Raina P, Santaguida P, Ismaila A, Patterson C, Cowan D, Levine M, Booker L, Oremus M (2008) Effectiveness of cholinesterase inhibitors and memantine for treating dementia: evidence review for a clinical practice guideline. *Ann Intern Med* 148:379–397
- Sağlık BN, İlgin S, Özkay Y (2016) Synthesis of new donepezil analogues and investigation of their effects on cholinesterase enzymes. *Eur J Med Chem* 124:1026–1040
- Sağlık BN, Kaya Çavuşoğlu B, Osmaniye D, Levent S, Acar Çevik U, İlgin S, Özkay Y, Kaplancıklı ZA, Öztürk Y (2019) In vitro and in silico evaluation of new thiazole compounds as monoamine oxidase inhibitors. *Bioorg Chem* 85:97–108
- Sang Z, Pan W, Wang K, Ma Q, Yu L, Liu W (2017a) Design, synthesis and biological evaluation of 3,4-dihydro-2(1H)-quinoline-O-alkylamine derivatives as new multipotent cholinesterase/monoamine oxidase inhibitors for the treatment of Alzheimer's disease. *Bioorg Med Chem* 25(12):3006–3017
- Sang Z, Wang K, Wang H, Wang H, Ma Q, Han X, Ye M, Yu L, Liu W (2017b) Design, synthesis and biological evaluation of 2-acetyl-5-O-(aminoalkyl)phenol derivatives as multifunctional agents for the treatment of Alzheimer's disease. *Bioorg Med Chem Lett* 27:5046–5052
- Scarpini E, Scheltens P, Feldman H (2003) Treatment of Alzheimer's disease: current status and new perspectives. *Lancet Neurol* 2(9):539–547
- Sterling J, Herzig Y, Goren T, Finkelstein N, Lerner D, Goldenberg W, Miskolczi I, Molnar S, Rantal F, Tamas T, Toth G, Zagyyva A, Zekany A, Finberg J, Lavian G, Gross A, Friedman R, Razin M, Huang W, Kraiss B, Cherev M, Youdim MB, Weinstock M (2002) Novel dual inhibitors of AChE and MAO derived from hydroxy aminoindan and phenethylamine as potential treatment for Alzheimer's disease. *J Med Chem* 45(24):5260–5279

- Takeda A, Loveman E, Clegg A, Kirby J, Picot J, Payne E, Green C (2006) A systematic review of the clinical effectiveness of donepezil, rivastigmine and galantamine on cognition, quality of life and adverse events in Alzheimer's disease. *Int J Geriatr Psychopharmacol* 21(1):17–28
- Tripathi RK, Ayyannan SR (2016) Design, synthesis, and evaluation of 2-amino-6-nitrobenzothiazole-derived hydrazones as MAO inhibitors: role of the methylene spacer group. *ChemMedChem* 11(14):1551–1567
- Tok F, Koçyigit Kaymakçioğlu B, Sağlık BN, Levent S, Özkay Y, Kaplancıklı ZA (2019) Synthesis and biological evaluation of new pyrazolone Schiff bases as monoamine oxidase and cholinesterase inhibitors. *Bioorg Chem* 84:41–50
- Wouters J (1998) Structural aspects of monoamine oxidase and its reversible inhibition. *Curr Med Chem* 5(2):137–162
- Xiao G, Li Y, Qiang X, Xu R, Zheng Y, Cao Z, Luo L, Yang X, Sang Z, Su F, Deng Y (2017) Design, synthesis and biological evaluation of 4'-aminochalcone-rivastigmine hybrids as multifunctional agents for the treatment of Alzheimer's disease. *Bioorg Med Chem* 25(3):1030–1041
- Xu YX, Wang H, Li XK, Dong SN, Liu WW, Gong Q, Wang TD, Tang Y, Zhu J, Li J, Zhang HY, Mao F (2018) Discovery of novel propargylamine-modified 4-aminoalkyl imidazole substituted pyrimidinylthiourea derivatives as multifunctional agents for the treatment of Alzheimer's disease. *Eur J Med Chem* 143:33–47
- Yan-Yan H (2010) An efficient synthesis of 3-(indol-3-yl)quinoxalin-2-ones with TfOH-Catalyzed Friedel-Crafts type coupling reaction in air. *Tetrahedron Lett* 51(15):2023–2028
- Youdim MB, Buccafusco JJ (2005) Multi-functional drugs for various CNS targets in the treatment of neurodegenerative disorders. *Trends Pharm Sci* 26(1):27–35
- Youdim MB, Edmondson D, Tipton KF (2006) The therapeutic potential of monoamine oxidase inhibitors. *Nat Rev Neurosci* 7(4):295–309